Stereochemical control of H_2O_2 dismutation by Hangman porphyrins†

Joel Rosenthal, Leng Leng Chng, Stephen D. Fried and Daniel G. Nocera*

Received (in Berkeley, CA, USA) 17th November 2006, Accepted 3rd May 2007
First published as an Advance Article on the web 23rd May 2007
DOI: 10.1039/b616884a

Incorporation of a disparate set of aryl groups appended to the *meso*-positions of Hangman porphyrin xanthene architectures dramatically impacts the ability of such systems to catalyze the disproportionation of H_2O_2 *via* the catalase reaction.

Oxygen activation by heme-iron centers is exploited by Nature for cellular energy production.[1–4] We have captured the fundamental O–O bond breaking reactivity that drives this energy liberating process using a Hangman porphyrin xanthene (HPX) construct.[5] The Hangman motif is embodied by the positioning of an acid-base group above a (P)Fe^{III}–OH (P = porphyrin) platform *via* a xanthene or dibenzofuran spacer. For such systems, the catalase and epoxidation reactivities of the protoporphyrin IX based class of proteins is emulated by using an acid functionality to unmask a high-valent metal-oxo *via* a proton-coupled electron transfer (PCET) process.[6] We have shown that optimization of the pK_a of the pendent acid group for Hangman architectures dramatically impacts the efficacy of PCET reactions,[7] but little is known about how the basal steric and electronic properties of the iron porphyrin platform impacts PCET reactivity. To address this issue, we now report a set of Hangman derivatives (**1–3**) that incorporate pendent aryl groups with varying stereochemical and electronic properties and assess which of these are paramount to the PCET activation of O–O bonds at the Hangman platform.

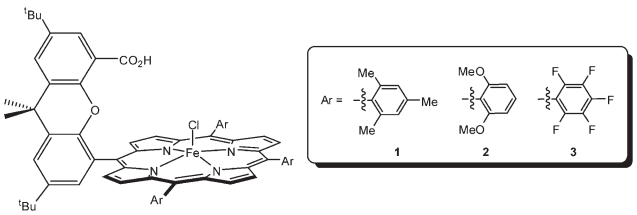

The strategy for the synthesis of porphyrin Hangman complexes **1–3** that is outlined in Scheme 1 borrows from that already described.[8] The protected xanthene acetal (**5**) is prepared from the symmetric xanthene dibromide (**4**) by lithiation and reaction with DMF to generate the bromoxanthene aldehyde, followed by subsequent condensation with neopentyl glycol. Lithiation of **5** followed by reaction with CO_2 and deprotection of the masked aldehyde with trifluoroacetic acid generates **6**. Esterification of the pendent carboxylic acid with methanol in the presence of H_2SO_4 provides aldehyde **7**, which can then be reacted with a variety of aryl aldehydes and pyrrole under standard Lindsey conditions to deliver freebase Hangman **8**. Hydrolysis under acidic conditions is necessary to convert the ester hanging group to the desired carboxylic acid functionality.‡

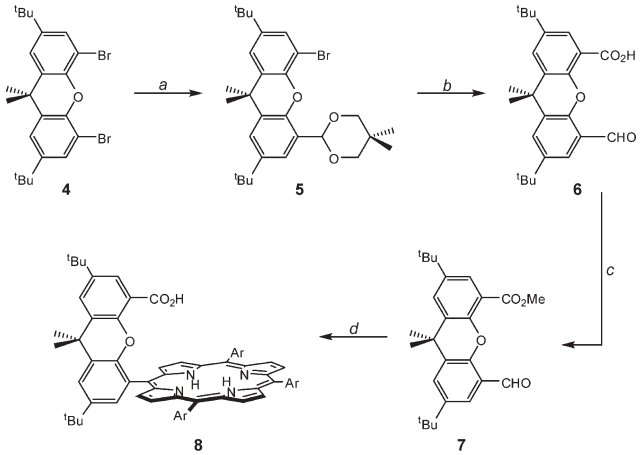

Scheme 1 (a) (i) Phenyllithium, C_6H_{12}–THF; (ii) DMF, H_2O; (iii) neopentyl glycol, benzenesulfonic acid, toluene, Δ; (b) (i) phenyllithium, C_6H_{12}–THF; (ii) CO_2; (iii) trifluoroacetic acid, water; (c) methanol, H_2SO_4, Δ; (d) (i) pyrrole, aryl aldehyde (Ar–CHO), $BF_3{\cdot}OEt_2$, $CHCl_3$; (ii) DDQ; (iii) AcOH, H_2SO_4, H_2O, Δ.

The crystal structure of the freebase precursor of **3**‡ is shown in Fig. 1. The structure is similar to other porphyrin Hangman derivatives.[9] Noteworthy structural features include the geometry of the xanthene spacer, which is canted by roughly 78° with respect to the porphyrin plane. Additionally, the xanthene pillar is slightly bent at the sp^3 hybridized carbon on the aromatic backbone by nearly 15°. Similar distortions have been observed for other porphyrin xanthene architectures.[9–11]

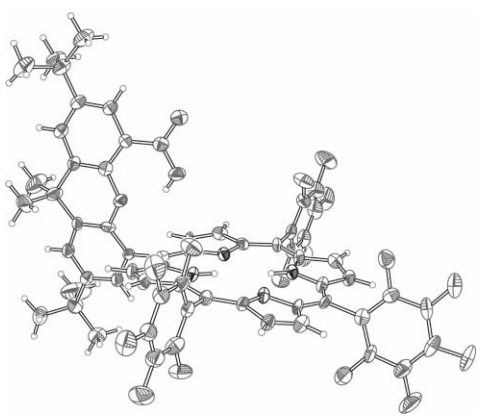

Fig. 1 Crystal structure of the freebase precursor to **3**. Ellipsoids shown at the 50% probability level.

Department of Chemistry, 6-335, Massachusetts Institute of Technology, Cambridge, MA 02139, USA. E-mail: nocera@mit.edu

† Electronic supplementary information (ESI) available: Tables for X-ray structure determination of the freebase precursor to **3**, and time course of the H_2O_2 dismutation for all compounds studied. See DOI: 10.1039/b616884a

Table 1 Reactivity data for H_2O_2 disproportionation

Compound	TOF/min^{-1}[a]	TON (% conversion)[b]
FeCl(TMP)	0.2 ± 0.1	162 ± 14 (30%)
FeCl(TMP)[c]	2.4 ± 0.4	236 ± 16 (44%)
1	102.3 ± 5.3	533 ± 8 (98%)
2	22.3 ± 1.3	160 ± 15 (31%)
3	27.2 ± 1.4	147 ± 6 (27%)

[a] TOF recorded over initial 30 seconds of reaction. [b] After 60 minute reaction time. [c] Addition of one equivalent $PhCO_2H$.

The disproportionation of H_2O_2 to generate 0.5 and 1.0 equivalents of O_2 and H_2O, respectively, is an important PCET process that is catalyzed by a wide variety of metalloproteins and enzymes.[12] With Hangman compounds **1–3** in hand, the structural and electronic factors that influence the O–O bond activation of the catalase transformation within the Hangman manifold can be assessed.

As shown in Table 1, the TON recorded for **1** surpasses 500 in less than 5 minutes for the Hangman complex, whereas the redox only porphyrin, FeCl(TMP) (TMP = 5,10,15,20-tetramesitylporphyrin), shows low activity for the disproportionation.§ The addition of external acid ($PhCO_2H$) enhances the TON observed for the control system, but the activity remains far below that observed for **1** in which intramolecular proton transfer from the pendent acid group converts a putative metal-bound hydroperoxide into a compound I type intermediate *via* a proton driven heterolytic O–O bond scission (Scheme 2).[5,13] This compound I species oxidizes a second equivalent of H_2O_2 to generate O_2 and an equivalent of H_2O.

We next probed the effect that modulation of the electronic and steric properties of the porphyrin ligand has on catalase activity. The redox chemistry of tetraarylporphyrins is perturbed significantly by altering the electronic properties of the ancillary aryl groups. For instance, the $P^{\bullet+}/P$ reduction potential of zinc(II) porphyrins shifts significantly along the series Ar = 2,6-dimethoxyphenyl ($E_{1/2}$ = 0.71 V *vs.* SCE)[14] < mesityl ($E_{1/2}$ = 0.98 V)[15] < pentafluorophenyl ($E_{1/2}$ = 1.20 V).[16]¶ Notwithstanding, the disparate electronic properties of **1–3** are not reflected in dramatic reactivity differences for H_2O_2 dismutation. As shown by the TOF and conversion percentages provided in Table 1, both the electron rich and poor Hangman systems (**2** and **3**, respectively) are less efficient dismutase catalysts as compared with the parent mesityl-based Hangman platform (**1**). Inspection of the reaction profiles for each of the catalysts of Table 1 (see Fig. S1 of ESI†) shows that each of the Hangman systems initially reacts rapidly with H_2O_2 to generate O_2 and then reaches a plateau. While the mesityl derivative (**1**) consumes all available H_2O_2 within several minutes, catalysts **2** and **3** begin to level off after roughly 90 seconds, producing roughly 150 and 135 turnovers over the course of the initial five minutes, respectively.

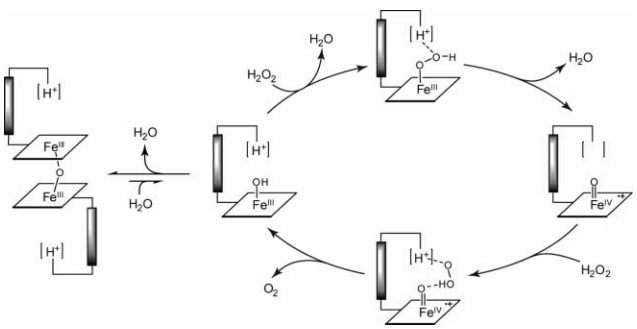

Scheme 2

Catalyst decomposition *via* oxidative processes may account for the lower TON observed for **2** and **3**. However, iron porphyrins are generally robust oxidation catalysts,[17] especially those incorporating fluorinated aryl groups on the porphyrin periphery such as Hangman **3**.[18,19] Accordingly, it is unlikely that the Hangman derivatives with fluorinated and dimethoxyphenyl groups would undergo oxidative degradation in the same way and at comparable rates. Another potential pathway for catalyst deactivation centers on the fact that heme-iron porphyrins may dimerize to generate diiron(III)-μ-oxo complexes. Porphyrins with ancillary 2,6-dimethoxyphenyl and pentafluorophenyl groups at the macrocycle *meso*-positions have been shown to form diiron(III)-μ-oxo dimers.[20–24] Moreover, both iron(III) chloride 5,10,15,20-(2,6-dimethoxylphenyl)porphyrin and iron(III) chloride 5,10,15,20-(pentafluorophenyl)porphyrin are virtually inactive H_2O_2 dismutase catalysts.‖ Conversely, tetraarylporphyrins with mesityl groups are too sterically encumbered to dimerize *via* a diiron(III)-μ-oxo linker. Indeed, mesityl appended porphyrins are one of the few cases in which a monomeric iron(III) hydroxide porphyrin derivative can be isolated and studied.[20] In line with this reasoning, FeCl(TMP) catalyzes H_2O_2 dismutation with lower initial TOF, as compared to Hangman derivatives **2** and **3**, but it remains active over longer time durations (Table 1, Fig. S1†). This is presumably because the mesityl groups prevent μ-oxo formation, which results in the formation of similar amounts of O_2 as compared to **2** and **3** over the course of 60 minutes. Evidence for the deactivation of **2** and **3** by μ-oxo dimerization was obtained from mass spectrometric analysis of Hangman porphyrins **1–3** in the presence of water and hydroxide. For the mesityl appended Hangman, only MS signals associated with the monomer are observed; however, for both **2** and **3**, dimerization products are observed.

As shown in Scheme 2, diiron(III)-μ-oxo dimerization subverts catalase activity by sending the system off the catalytic pathway. For the case of the mesityl Hangman (**1**), this equilibrium lies exclusively to the right (monomer) and, as a result, the initial TOF and total TON after 60 minutes of reaction time are large. By contrast, this equilibrium should lie far toward the left for Hangman derivatives with 2,6-dimethoxyphenyl or pentafluorophenyl substituents (**2** and **3**). This cycle explains our observations, since the initial TOF values recorded for **2** and **3** are relatively high, as compared to control compounds lacking a pendent acid group. However, this initial activity diminishes in time. Conversion of the iron(III) Hangman systems to diiron(III)-μ-oxo dimers during the course of the catalase reaction ultimately leads to catalyst deactivation, thus accounting for the relatively low TON at longer reaction times.

In summary, while it is possible to tune the electronic properties of Hangman porphyrin architectures by incorporating a disparate set of aryl groups about the macrocycle periphery, steric effects associated with the prevention of diiron(III)-μ-oxo dimerization are crucial to the efficacy of such systems in catalyzing oxygen activation chemistry. Also of note is the realization that the proximal hydrogen-bonding network enforced by the Hangman

motif is not sufficient in and of itself to stabilize a monomeric iron(III) hydroxide porphyrin.[6] Indeed, in addition to a hydrogen-bonding manifold, decoration of the porphyrin periphery with aryl groups with the appropriate stereoelectronic properties is required for the development of highly active and robust systems for O–O bond activation and oxidation catalysis.

This work was supported by the National Institutes of Health (GM 47274). J. R. thanks the Fannie and John Hertz Foundation for a doctoral fellowship. The authors thank Dr D. R. Manke for assistance with crystallography and D. Wright for uplifting achievements.

Notes and references

‡ The synthesis of Hangman porphyrins **1** and **2** and synthetic precursor **7** have been reported previously.[3,6] The synthesis of Hangman porphyrin **3** was accomplished as follows: a mixture of xanthene aldehyde **7** (0.10 g, 0.25 mmol), pentafluorobenzaldehyde (0.735 g, 3.75 mmol) and pyrrole (0.275 mL, 4.0 mmol) in chloroform (425 mL) was purged with nitrogen for 45 min, after which a portion of $BF_3{\cdot}OEt_2$ (0.168 mL, 1.32 mmol) was added *via* syringe. The solution was stirred at room temperature under nitrogen in the dark for 1 h and 2,3-dichloro-5,6-dicyano-1,4-benzoquinone (0.68 g, 3.0 mmol) was added to the reaction. After stirring for an additional hour under nitrogen, the solvent was removed under reduced pressure. The dark residue was redissolved in dichloromethane (100 mL) containing 2% triethylamine and filtered through celite. The filtrate was loaded directly onto a silica gel column and eluted with dichloromethane until no more porphyrinic product was detected by analytical TLC. Further purification by column chromatography on silica was accomplished using hexanes and dichloromethane (5 : 2) as the eluent to give the porphyrin ester as a violet microcrystalline solid (87 mg, 31% yield based on starting aldehyde). The purified porphyrin ester (80 mg, 0.0676 mmol) was dissolved in a mixture of acetic acid (20 mL) and sulfuric acid (5 mL). Water (6.0 mL) was added to the green solution and the reaction was refluxed under N_2 in the dark for 7 days. The reaction was cooled to room temperature and extracted with 50 mL of dichloromethane. The organic layer was washed with water, dried over Na_2SO_4, and the solvent was removed by rotary evaporation. Purification by column chromatography on silica was accomplished using dichloromethane as the eluent to provide the freebase precursor to Hangman porphyrin **3** as a purple solid in near quantitative yield. ^{1}H NMR (500 MHz, $CDCl_3$, 25 °C): δ = 8.91 (m, 5H), 8.79 (d, J = 7 Hz, 2H), 8.09 (d, J = 4 Hz, 1H), 7.98 (d, J = 4 Hz, 1H), 7.72 (d, J = 4 Hz, 1H), 7.62 (d, J = 4 Hz, 1H), 1.99 (s, 6H), 1.57 (s, 9H), 1.25 (s, 9H), −2.76 (s, 2H). HRESIMS (MH^+) calcd for $C_{62}H_{39}F_{15}N_4O_3$ m/z = 1173.2855; found, 1173.2854.

Iron insertion into the freebase Hangman described above was accomplished as follows: a combination of the freebase Hangman (60 mg, 0.51 mmol), $FeBr_2$ (350 mg), and CH_3CN (30 mL) was refluxed under nitrogen for 8 h, opened to air, and brought to dryness under vacuum. The solids were redissolved in dichloromethane (100 mL) and washed with water (4 × 75 mL). The organic layer was stirred with 20% HCl (50 mL) for 75 min, washed with water (5 × 100 mL), and taken to dryness. The resulting residue was purified by column chromatography on silica gel, eluting first with dichloromethane to remove less polar impurities and then with 5% methanol in dichloromethane to elute the product. Following concentration of the product under reduced pressure, the dark brown material was re-treated with HCl as described above to furnish **3** as a brown powder (48 mg, 84% yield). HRFABMS ($[M - Cl]^+$) calcd for $C_{71}H_{70}N_4O_3Fe$ m/z = 1082.4797; found, 1082.4773. Anal. calcd for $C_{71}H_{70}ClN_4O_3Fe$: C, 76.23; H, 6.31; N, 5.01. Found: C, 76.44; H, 6.19; N, 4.82%.

Crystal data: freebase precursor to **3**: $C_{62}H_{39}F_{15}N_4O_3$, M = 1172.97, orthorhombic, space group $Pca2_1$, a = 23.784(3), b = 14.5290(16), c = 16.258(2) Å, U = 5618.1(12) Å^3, Z = 4, D_c = 1.387 Mg m^{-3}, T = 183(2) K, μ = 0.120 mm^{-1}, w$R2$ = 0.1842 (5035 independent reflections), $R1$ = 0.0708 [$I > 2\sigma(I)$]. CCDC 628103. For crystallographic data in CIF or other electronic format, see DOI: 10.1039/b616884a

§ *Hydrogen peroxide disproportionation reactions*: dismutation reactions were performed at room temperature in a sealed (PTFE septum) 10 mL reaction vial equipped with a magnetic stirbar and a capillary gas delivery tube linked to a graduated burette filled with water. The reaction vial was charged with 1 μmol of the iron porphyrin catalyst, 25 μmol of 1,5-dicyclohexylimidazole, 1.5 mL of CH_2Cl_2, and 0.5 mL of CH_3OH. The solution was stirred for 5–10 minutes to ensure gas pressure equilibration. An aliquot of 10.4 M (30%) aqueous H_2O_2 (0.11 mL) was added to the reaction mixture *via* syringe, and the reaction mixture was stirred vigorously. The time was set to zero immediately after addition of H_2O_2. The conversion of the reaction was monitored volumetrically, and the TON for produced O_2 (n) was calculated through the perfect gas equation $pV = nRT$, assuming that p = 1 atm. The identity of the oxygen gas was confirmed independently by the alkaline pyrogallol test.

¶ All oxidation potentials recorded in CH_2Cl_2 *vs.* SCE using tetrabutylammonium perchlorate (TBAP) or tetrabutylammonium hexafluorophosphate ($TBAPF_6$) as the electrolyte.

‖ Control H_2O_2 disproportionation experiments employing iron(III) chloride 5,10,15,20-(2,6-dimethoxylphenyl)porphyrin and iron(III) chloride 5,10,15,20-(pentafluorophenyl)porphyrin both result in the production of negligible amounts of O_2 under the conditions described above.§

1 C. W. Hoganson, M. A. Pressler, D. A. Proshlyakov and G. T. Babcock, *Biochim. Biophys. Acta*, 1998, **1365**, 170–174.
2 J. E. Morgan and M. Wilkstrom, *Biochemistry*, 1991, **30**, 948–958.
3 B. E. Schultz and S. I. Chan, *Annu. Rev. Biophys. Biomol. Struct.*, 2001, **30**, 23–65.
4 B. Kadenbach, *Biochim. Biophys. Acta*, 2003, **1604**, 77–94.
5 C. J. Chang, L. L. Chng and D. G. Nocera, *J. Am. Chem. Soc.*, 2003, **125**, 1866–1876.
6 C. J. Chang, M. C. Y. Chang, N. H. Damrauer and D. G. Nocera, *Biochim. Biophys. Acta*, 2004, **1655**, 13–28.
7 L. L. Chng, C. J. Chang and D. G. Nocera, *Org. Lett.*, 2003, **5**, 2421–2424.
8 C. J. Chang, C. Y. Yeh and D. G. Nocera, *J. Org. Chem.*, 2002, **67**, 1403–1406.
9 C. Y. Yeh, C. J. Chang and D. G. Nocera, *J. Am. Chem. Soc.*, 2001, **123**, 1513–1514.
10 J. Rosenthal and D. G. Nocera, *Prog. Inorg. Chem.*, **55**, in press.
11 C. K. Chang, N. Bag, B. Guo and S. M. Peng, *Inorg. Chim. Acta*, 2003, **351**, 261–268.
12 P. Nicholls, I. Fita and P. C. Loewen, *Adv. Inorg. Chem.*, 2000, **51**, 51–106.
13 J. L. Dempsey, A. J. Esswein, D. R. Manke, J. Rosenthal, J. D. Soper and D. G. Nocera, *Inorg. Chem.*, 2005, **44**, 6879–6892.
14 J. Seth, V. Palaniappan, T. E. Johnson, S. Prathapan, J. S. Lindsey and D. F. Bocian, *J. Am. Chem. Soc.*, 1994, **116**, 10578–10592.
15 J. Otsuki, T. Narita, K. Tsutsumida, M. Takatsuki and M. Kaneko, *J. Phys. Chem. A*, 2005, **109**, 6128–6134.
16 A. Sena and V. Krishnana, *J. Chem. Soc., Faraday Trans.*, 1997, **93**, 4281–4288.
17 J. T. Groves, K. Shalyaev and J. Lee, in *The Porphyrin Handbook*, ed. K. M. Kadish, K. M. Smith and R. Guilard, Academic Press, New York, 2000, pp. 17–40.
18 C. K. Chang and F. J. Ebina, *J. Chem. Soc., Chem. Commun.*, 1981, 778–779.
19 P. S. Traylor, D. Dolphin and T. G. Traylor, *J. Chem. Soc., Chem. Commun.*, 1984, 279–280.
20 C. J. Chang, Z. H. Loh, C. Shi, F. C. Anson and D. G. Nocera, *J. Am. Chem. Soc.*, 2004, **126**, 10013–10020.
21 K. Jayaraj, A. Gold, G. E. Toney, J. H. Helms and W. E. Hatfield, *Inorg. Chem.*, 1986, **25**, 3516–3518.
22 R. J. Cheng, L. Latos-Grazynski and A. L. Balch, *Inorg. Chem.*, 1982, **21**, 2412–2418.
23 J. Rosenthal, B. J. Pistorio, L. L. Chng and D. G. Nocera, *J. Org. Chem.*, 2005, **70**, 1885–1888.
24 J. Rosenthal, D. Luckett, J. M. Hodgkiss and D. G. Nocera, *J. Am. Chem. Soc.*, 2006, **128**, 6546–6547.

